ON THE ORIGIN OF THE IRON K LINE IN THE SPECTRUM OF THE GALACTIC X-RAY BACKGROUND

Azita Valinia[1,2], Vincent Tatischeff[3], Keith Arnaud[1,2], Ken Ebisawa[1,4], and Reuven Ramaty[1]

Accepted for Publication in the Astrophysical Journal

ABSTRACT

We propose a mechanism for the origin of the Galactic ridge X-ray background that naturally explains the properties of the Fe K line, specifically the detection of the centroid line energy below 6.7 keV and the apparent broadness of the line. Motivated by recent evidence of nonthermal components in the spectrum of the Galactic X-ray/γ-ray background, we consider a model that is a mixture of thermal plasma components of perhaps supernova origin and nonthermal emission from the interaction of low energy Cosmic ray electrons (LECRe) with the interstellar medium. The LECRe may be accelerated in supernova explosions or by ambient interstellar plasma turbulence. Atomic collisions of fast electrons produce characteristic nonthermal, narrow X-ray emission lines that can explain the complex Galactic background spectrum. Using the ASCA GIS archival data from the Scutum arm region, we show that a two-temperature thermal plasma model with $kT \sim 0.6$ and ~ 2.8 keV, plus a LECRe component models the data satisfactorily. Our analysis rules out a purely nonthermal origin for the emission. It also rules out a significant contribution from low energy Cosmic ray ions, because their nonthermal X-ray production would be accompanied by a nuclear γ-ray line diffuse emission exceeding the upper limits obtained using OSSE, as well as by an excessive Galaxy-wide Be production rate. The proposed model naturally explains the observed complex line features and removes the difficulties associated with previous interpretations of the data which evoked a very hot thermal component ($kT \sim 7$ keV).

[1]Laboratory for High Energy Astrophysics, Code 662, NASA/Goddard Space Flight Center, Greenbelt, MD 20771; valinia@milkyway.gsfc.nasa.gov

[2]Department of Astronomy, University of Maryland, College Park, MD 20742

[3]Center de Spectrométrie Nucléaire et de Spectrométrie de Masse, IN2P3-CNRS, 91405 Orsay, France

[4]USRA

Subject headings: galaxies: individual (Milky Way) — ISM: structure — X-rays: ISM — cosmic rays — supernova remnants

1. INTRODUCTION

The origin of the Galactic X-ray background has remained a puzzle since its discovery during the pioneering rocket experiments of Bleach et al. (1972). Since then, X-ray emission from the Galactic plane and, in particular, the ridge (the narrow region around the Galactic center covering from $\pm 60^\circ$ in longitude and $\pm 10^\circ$ in latitude) has been studied with every major X-ray observatory. Below 10 keV, the spectrum is rich in emission lines from Fe, Mg, Si and S (e.g. Kaneda et al. 1997; hereafter K97). Above 10 keV, a power law component is clearly detected (e.g. Yamasaki et al. 1997; Valinia & Marshall 1998) with an exponential cutoff near 40 keV (Valinia, Kinzer & Marshall 2000, hereafter VKM00).

Both diffuse and discrete sources have been proposed for the origin of this emission. RS CVn binaries and Cataclysmic Variables (CVs) have been considered as significant contributors to the emission below 10 keV. However, Ottmann & Schmitt (1992) have estimated that only 1% of the iron K line detected in the unresolved Galactic background spectrum is due to RS CVns. Kaneda (1997) has shown that in order for CVs to make up the diffuse emission, their space density would have to be a factor of 100 larger than previously estimated (Patterson 1984). Recently, from the analysis of ROSAT PSPC data, Tanaka, Miyaji & Hasinger (1999) have shown that a class of hard sources with $L_X \sim 10^{29-30}\,\mathrm{erg\,s^{-1}}$ and as abundant as stellar coronal sources is required to account for the unresolved ridge emission. No such class of sources has been identified.

The discovery using *Tenma* of the iron K line in the ridge spectrum motivated the idea that the emission below 10 keV is due to a diffuse, hot, optically-thin plasma of temperature 5–15 keV (Koyama et al. 1986). Later, high resolution measurements of the ridge spectrum using ASCA revealed a complex emission line structure. The ASCA spectrum cannot be satisfactorily modeled with a single thermal component in ionization equilibrium (K97). Instead, K97 modeled the emission by two non-equilibrium ionization components with temperatures of ~ 0.8 and 7 keV. While this model provides a good fit to the spectrum, it is difficult to explain the production and confinement of such hot gas uniformly permeating the interstellar medium (ISM). Supernova remnant shock temperatures reach only about 3 keV. Also, the 7 keV temperature exceeds the gravitational potential of the disk by at least one order of magnitude (Townes 1989). Therefore, according to this model, the hot gas must be constantly and uniformly replenished in the Galaxy. To overcome this difficulty, Tanuma et al. (1999) consider heating and confinement of the plasma in the Galactic plane via magnetic reconnection. They numerically investigate how magnetic reconnection triggered by supernova explosions heats the plasma which is consequently confined in magnetic islands. They conclude that for this mechanism to work, local magnetic fields of $\sim 30\,\mu$G are necessary. This model implies that the hot plasma must be very localized.

Another problem with the purely thermal scenario is that the two-temperature model can not account for the data above 10 keV, which require at least one additional component at higher energies. Simultaneous RXTE and OSSE observations up to 1 MeV show the presence of an additional component in the spectrum that can be characterized as an exponentially cut-off power law (VKM00). This component dominates in the 10-400 keV band and contributes approximately 35% of the total 3-10 keV emission. VKM00 estimated that up to $\sim 50\%$ of the emission at 60 keV is due to discrete sources, with the rest remaining unresolved. These results imply that there is a nonthermal contribution to the Galactic ridge emission below 10 keV. This paper explores some of the consequences.

The unresolved hard X-ray/soft γ-ray diffuse component detected by RXTE and OSSE can be produced either by bremsstrahlung from low energy Cosmic ray electrons (< 1 MeV; LECRe) or inverse Compton scattering off ultra-relativistic ($\sim$0.1-10 GeV) electrons (e.g. Skibo & Ramaty 1993). However, Skibo, Ramaty & Purcell (1996) have shown that the emission up to 100 keV is more likely of electron bremsstrahlung origin, because a large population of ultra-relativistic electrons would also produce a significant Galactic synchrotron radio emission at $\sim$100 Mhz and this is not observed. In addition to the bremsstrahlung continuum, LECRe produce nonthermal narrow X-ray emission lines below 10 keV via K-shell vacancy creation in ambient heavy atoms. Low energy Cosmic ray ions (LECRi) also produce characteristic broad and narrow X-ray emission lines (Tatischeff, Ramaty & Kozlovsky 1998 and references therein, Dogiel et al. 1998). Their contribution to the Galactic ridge diffuse emission has been considered by Tatischeff, Ramaty & Valinia (1999) and Tanaka, Miyaji & Hasinger (1999). However, we show in §4 that LECRi can not account for the Galactic X-ray background because their nonthermal X-ray production would be accompanied by a nuclear γ-ray line diffuse emission exceeding the upper limits obtained using OSSE, as well as by an unreasonably high Galaxy-wide Be production rate. For these reasons, we focus on the role of low energy Cosmic ray electrons in nonthermal X-ray production below 10 keV.

In this paper, we report on the analysis of ~ 111 ks archival ASCA data from the Scutum arm region on the Galactic plane. Instead of applying non-equilibrium ionization models, we show that an alternative model, namely nonthermal X-rays from the interaction of LECRe with the ISM plus two thermal plasma components (of ~ 2.8 keV and 0.6 keV) produces an equally good fit to the spectrum. According to our best fit model, the thermal and nonthermal components contribute 81% and 11%, respectively, of the $0.6 - 9$ keV emission, with the remaining emission contributed by the Cosmic X-ray background. (In the 4-9 keV band, the thermal and nonthermal components contribute 38% and 36%, respectively.) In §2 we investigate the X-ray line and continuum emission from the interaction of LECRe with the ISM. In §3 we present the data and our analysis and in §4 we discuss the implications of our results.

2. X-RAYS FROM LECRe INTERACTION WITH THE ISM

In the LECRe scenario, nonthermal X-ray line emission results from the filling of inner-shell vacancies produced by the fast electrons in the ambient atoms. We assumed the X-ray production region to be neutral and of solar composition (Anders & Grevesse 1989) and considered the Kα and Kβ lines from ambient C, N, O, Ne, Mg, Si, S, Ar, S and Fe. The transition energies are given in Tatischeff et al. (1998, Table 6). The X-ray line production cross section can be written as

$$\sigma_{Line} = \sigma_I w k, \tag{1}$$

where σ_I is the cross section for the collisional ionization leading to the K-shell vacancy, w is the fluorescence yield for the K shell (Krause 1979) and k is the relative line intensity among the possible transitions which can fill the inner-shell vacancy (Salem, Panossian, & Krause 1974). For the K-shell ionization cross section, we used the semiempirical formula of Quarles (1976), which is in good agreement with the data compiled in Long et al. (1990). Since the intrinsic width of the X-ray lines is smaller than the ASCA energy resolution, the determination of the exact line profiles is beyond the scope of this paper. For simplicity, we adopted the same width for all the lines, ΔE_X=10 eV, which is the approximate width of the 6.40 keV Fe line in a cold ambient medium (Dogiel et al. 1998).

X-ray continuum emission is essentially due to bremsstrahlung from the fast primary electrons. We estimated bremsstrahlung from knock-on secondary electrons to be of minor importance above 0.5 keV. We considered primary electron bremsstrahlung in ambient H and He and calculated the corresponding differential cross sections from equation (3BN) in Koch & Motz (1959).

The differential X-ray production rate can be written as

$$\frac{dQ}{dE_X} = \sum_j n_j \int_0^\infty J_e(E) v(E) \frac{d\sigma_j}{dE_X}(E_X, E) dE \ , \tag{2}$$

where n_j is the density of the ambient isotope j, $J_e(E)$ is the differential equilibrium electron number as a function of the electron kinetic energy E, $v(E)$ is the electron velocity and $d\sigma_j/dE_X$ is the differential X-ray production cross section for electron interactions with particles of type j. We perform calculations with an electron equilibrium spectrum of the form

$$J_e(E) \propto E^S e^{-E/E_0} \ . \tag{3}$$

Figure 1 shows the X-ray emission produced by a LECRe population with S=0.3 and E_0=90 keV, which provides a good fit to the RXTE and OSSE Scutum arm data

(see §3). The calculations are normalized to a total kinetic energy in the fast electrons E_{tot}=$\int_0^\infty EJ_e(E)dE$=1 erg and an average ambient H density of 1 atom cm^{-3}. The spectral index S=0.3 could be due to the injection of electrons of energies $\gtrsim E_0$ into the neutral phase of the ISM. Indeed, the equilibrium electron spectrum would then satisfy

$$J_e(E < E_0) = \frac{1}{dE/dt} \int_{E_0}^{\infty} \frac{dN_e}{dt}(E')dE' \propto \frac{1}{dE/dt} \ , \tag{4}$$

where dN_e/dt is the electron source spectrum (it is assumed that $dN_e/dt(E) = 0$ for $E < E_0$) and dE/dt is the electron energy loss rate in a neutral ambient medium, which is roughly proportional to $E^{-0.3}$ below ∼100 keV (Berger & Seltzer 1982). As shown in Figure 1, the continuum emission is accompanied by strong X-ray lines in the ASCA energy range.

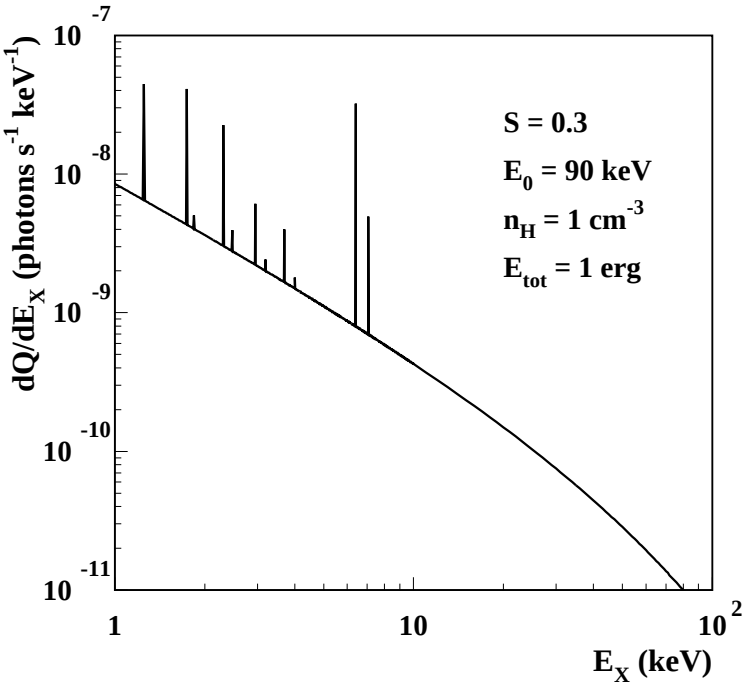

Fig. 1.— Nonthermal X-ray emission produced by LECRe with S=0.3 and E_0=90 keV (eq. [3]) interacting in a neutral ambient medium of solar composition. The differential X-ray production rate is normalized to an average ambient H density of 1 atom cm^{-3} and a total electron kinetic energy of 1 erg.

3. OBSERVATIONS AND ANALYSIS

We used archival ASCA GIS data of the on-plane (i.e. $b \sim 0°$) Scutum arm region from Galactic longitude $26°.5 < l < 30°.0$. Overall, 10 pointings with a total good time exposure

of ~ 111 ks were used. These observations were performed from 1993 to 1997. For spectral analysis, data from the central region of the GIS with radius less than $22'$ was used, as this is the default cut-off radius in the ASCA Standard Processing Products. Within this radius, spectral resolution is known to be uniform, and the long term gain change and positional gain variation is calibrated within $\pm 1\%$ (Makishima et al. 1996).

The average count rate in the 0.5-10 keV band after removing point sources was $0.526\,\mathrm{cts\,s^{-1}}$ for GIS2 and $0.559\,\mathrm{cts\,s^{-1}}$ for GIS3. We were not able to make significant use of SIS data since fewer photons were collected by those instruments (the field of view for the SIS being much smaller than that for the GIS) and furthermore the degradation of the SIS response in later observations reduced the utility of that instrument.

Since the emission region is larger than the GIS field-of-view, "stray light effects" have to be taken into account. For the purpose of this analysis, an XRT response (i.e. ancillary response file or ARF) has been constructed by taking into account the stray-light effects up to $1^\circ.5$ from the XRT axis. The procedure is as follows. We randomly generated one-million X-ray photons within $1^\circ.5$ of the optical axis, and using ray-tracing calculated the number of photons which reached the detector plane. We repeated this procedure for 300 monochromatic energies from 0.1 to 12 keV. From these ray-traced images, taking account of the GIS detector response, we calculated the ARF for the diffuse emission corresponding to the detector region used (which excluded any point sources). For each energy bin,

$$\mathrm{ARF(cm^2str)} \propto \mathrm{S(cm^2)} \times \Omega\mathrm{(str)} \times \frac{N}{10^6}, \tag{5}$$

where S is the geometrical opening area of the ASCA X-ray telescope ($826.64\,\mathrm{cm^2}$), Ω is the solid angle of the assumed spatial extent (2.153×10^{-3} str), and N is the number of photons to have reached the detector region concerned. This is basically the same method described in K97.

We also calculated the diffuse ARF for a more realistic distribution of the emission along the Galactic plane. We assumed that the spatial distribution of emission was Gaussian in latitude with a 4° FWHM (as measured by Valinia & Marshall 1998) and constant in longitude. We found an insignificant difference in the best fit model parameters with the two different ARFs. In what follows we show results obtained with the ARF made assuming uniform emission from a circle of radius $1^\circ.5$.

Since the Cosmic X-ray background (CXB) is absorbed by the Galactic plane at energies below ~ 5 keV, we subtracted only the instrumental background from the data and included the CXB as a fixed component in the model. Archival night earth observations were used to determine the instrumental background. From the analysis of the blank sky GIS2 and GIS3 archival data, we found that the CXB was best fitted with a power law

function $k(E/1\ \mathrm{keV})^{-\Gamma}$. The best fit parameters were $\Gamma \sim 1.4$ and $k = 0.0177$ and 0.0192 photons $\mathrm{cm}^{-2}\,\mathrm{s}^{-1}\,\mathrm{keV}^{-1}$ at 1 keV for GIS2 and GIS3, respectively. In all the fits reported below the CXB component was absorbed by the best-fit Galactic hydrogen column. We simultaneously fit the GIS2 and GIS3 spectra. Because the emission is faint, we found that many channels were short of the $\sim$ 20 counts minimum required to yield meaningful χ^2 statistics. Therefore, before fitting the data, we binned channels 0-511 by a factor of 2 and channels 512-1023 by a factor of 8. This resulted in at least 20 counts in each bin.

Since the complex shape of the Fe K line is the prime focus of this paper, we first analyzed the 4-9 keV data (the channels above 9 keV have insufficient counts to be worth including in the fit). At these energies, the spectrum is little affected by the absorption due to the Galactic hydrogen column density. Our first attempt was to model the data using a single thermal plasma component (the mekal model; Mewe, Gronenschild, & van den Oord 1985; Mewe, Lemen, & van den Oord 1986; Kaastra 1992) absorbed by the Galactic plane. We derived a best fit temperature of $kT = 4.7\pm1.0$ keV. The result of this fit is shown in Figure 2a. The fit around the Fe K line is very poor. Therefore, we modeled the data using a thermal bremsstrahlung plus a Gaussian line component, as was also done by K97. The result of this with a best fit temperature parameter of $kT = 7.4^{+2.8}_{-2.3}$ keV is shown in Figure 2b. Notice that the quality of the fit around the Fe K line has dramatically improved but the width (187±59 eV) suggests that the line is intrinsically broad. Also, the peak line energy is detected at 6.627 ± 0.035 keV, a lower energy than that expected from a plasma in ionization equilibrium.

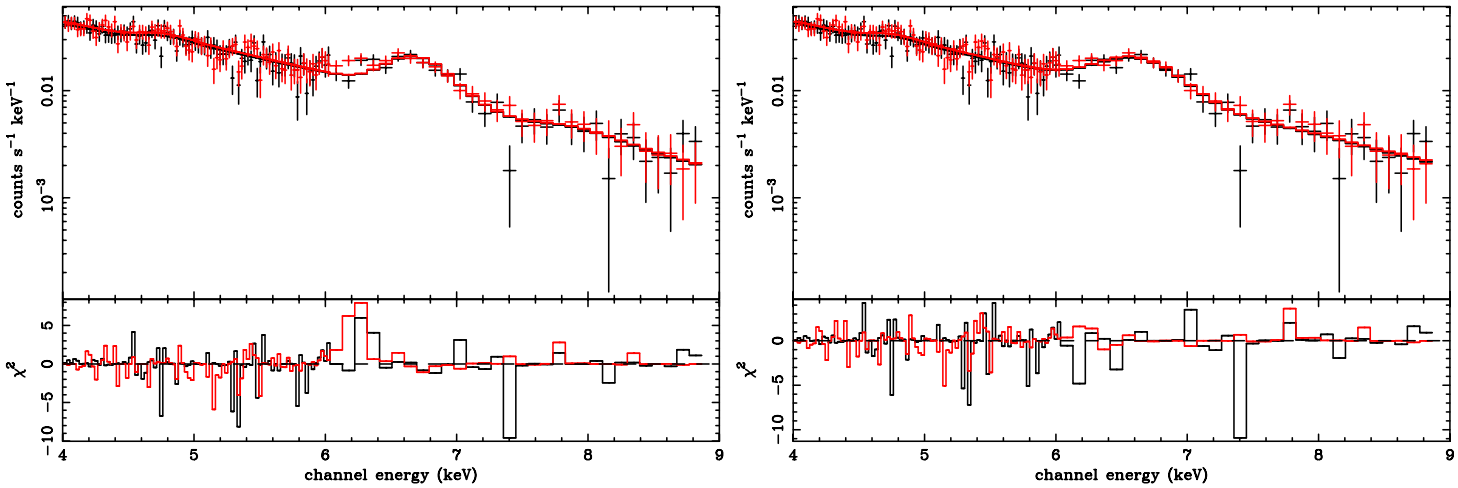

Fig. 2.— (a) ASCA GIS2 and GIS3 data fitted to an absorbed mekal model (left panel). (b) Same data as in (a) fitted to an absorbed bremsstrahlung plus Gaussian model (right panel).

Next, we modeled the data with the nonthermal LECRe component. However, since

the parameters of this component are directly related to the emission above 10 keV, we *first* used the RXTE and OSSE Scutum arm measurements of VKM00 to constrain the shape of the electron equilibrium spectrum (i.e. S and E_0 in eq. 3). VKM00 modeled the 3-400 keV spectrum with an absorbed thermal model plus an exponentially cutoff power law. We replaced the exponentially cutoff power law with the LECRe model and found that any spectral index $S > 0$ provided equally satisfactory fits to the data. We fixed the spectral index at $S = 0.3$, consistent with the scenario that accelerated electrons of energies $\gtrsim E_0$ are injected into a neutral medium (see §2). For the exponential turn-over energy, we found a best fit $E_0 \sim 90$ keV. The best fit result is obtained when it is assumed that the broad band diffuse emission has a spatial Gaussian distribution of FWHM $\lesssim 0°.5$ which is consistent with the interpretation that the hard X-ray/soft γ-ray emission is confined to a $\lesssim 1°$ thin disk centered roughly on the Galactic midplane. Indeed, from the RXTE survey of the Galactic plane, Valinia & Marshall (1998) find two spatial components for the diffuse emission: a thin disk of full width $\lesssim 0°.5$ centered roughly on the Galactic midplane and a broad component of Gaussian distribution with FWHM of about 4°. Moreover, this is consistent with the observation that the Fe K line is either extremely weak or not detected at all in ASCA measurements of the Galactic plane diffuse emission at high latitudes, $l > |1°|$ (K97). K97 also found that the scale height of the hard X-ray component was smaller than that of the soft component.

Using the parameters for the LECRe model obtained from the high energy data ($S = 0.3$, $E_0 = 90$ keV), we fit the 4-9 keV ASCA data with an absorbed LECRe model. However, this model did not produce a satisfactory fit to the data. In particular, the quality of the fit around the Fe K line was very poor. We then modeled the data with an absorbed LECRe plus a thermal plasma component. This provides a satisfactory fit to the entire energy range, including the Fe K line. This line appears to be broadened and shifted to 6.6 keV because it is a combination of the 6.4 keV LECRe line and the 6.7 keV from He-like Fe. Because the thermal plasma component has a temperature of ~ 3 keV there is a negligible contribution from the 6.97 keV line of H-like Fe. The parameters of this fit are shown in the top panel of Table 1.

Extending this model down to 0.6 keV, we found that it provided a good fit to the data only in the 2-9 keV band. Below 2 keV, the data significantly exceeded the model, requiring an additional low temperature component. Adding a second thermal plasma component to the above model and fitting for the best parameters yielded a good fit to the overall spectrum. The parameters of this model are given in the bottom panel of Table 1. These results suggest that there is a nearby low-temperature thermal component ($kT \sim 0.6$ keV) which accounts for the soft X-ray emission of the Galactic background (as implied by the low value of the hydrogen column density). The hard X-ray component (i.e. $E > 2$ keV) is

produced from superposition of a thermal component ($kT \sim 2.8$ keV gas) and a nonthermal LECRe component, absorbed through a larger hydrogen column. Figure 3a shows the data and folded model. Figure 3b shows the unfolded spectrum and model components.

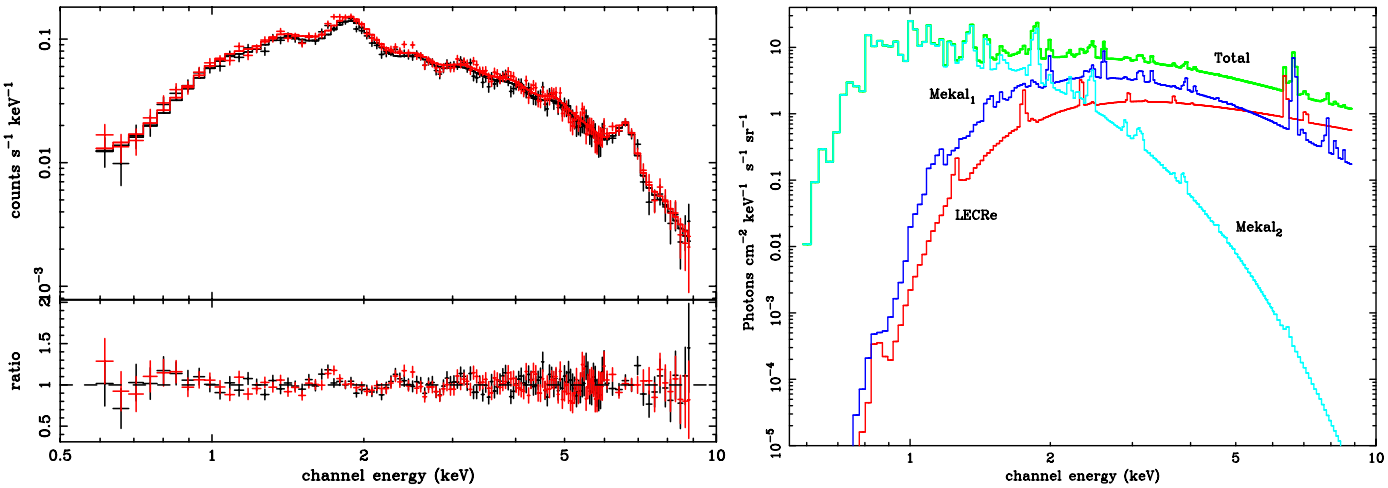

Fig. 3.— (a) Data and folded model in our favorite emission scenario summarized in Table 1 are shown. The lower window shows the ratio of data divided by the folded model (left panel). (b) Unfolded spectrum and model components. The CXB is included in the model but not shown for clarity of the plot (right panel).

4. DISCUSSION

The composite thermal plus LECRe model in Table 1 provides the best fit to the ASCA data. In this scenario, most of the emission below 2 keV is due to a thermal plasma component at $kT \sim 0.6$ keV. The hard X-ray emission above 2 keV is due to a combination of a hotter plasma component at $kT \sim 2.8$ keV, which may have been shock heated in supernova explosions, and a LECRe component which may also be related to supernova explosions, and which would account for part of the RXTE and OSSE data above 10 keV. We have assumed that this component is limited to the central 1° of the Galactic plane. This model produces a very good fit to the overall spectrum and, in particular, to the Fe K line complex. This is because the apparent broadening and shift in the mean energy of the Fe K line is produced by a combination of the thermal lines from de-excitation in He-like Fe and the nonthermal lines, primarily at 6.4 keV, due to K-shell vacancy production in ambient neutral Fe.

The ASCA SIS should be able to resolve the nonthermal 6.4 keV line from the thermal lines at ~ 6.7 keV. However, for the Scutum arm region the signal-to-noise is not sufficient to draw any conclusions. K97 have summed ASCA SIS data over a larger latitude range in

order to have enough counts to examine the shape of the Fe K line. They found clear evidence for photons with energies below that of the He-like line at ~ 6.7 keV and no evidence of emission at 6.4 keV. However, since the LECRe are likely confined close to the plane we expect any 6.4 keV line to be diluted in the K97 data. The photons with energies below that from the He-like line are from lower-ionization stages of Fe and are not predicted by thermal emission from a collisional plasma. As K97 correctly pointed out, this is good evidence for plasma that is out of ionization equilibrium. We differ from K97 in not requiring as high a continuum temperature so the plasma can be closer to equilibrium.

The RXTE and OSSE Scutum arm data above 10 keV are best modeled by a hard electron equilibrium spectrum ($S > 0$) which could result from the injection of electrons accelerated in a low-density ionized medium into a denser neutral medium in which they would produce most of the nonthermal X-rays. Assuming an average H density of $1\,\mathrm{cm}^{-3}$ in the X-ray production region, we calculated that a total electron kinetic energy of $2.9 \times 10^{53}\,\mathrm{erg}$ is needed to produce the 0.6-9 keV luminosity in the LECRe component of $2.5 \times 10^{37}\,\mathrm{erg\,s}^{-1}$ (Table 1). Dividing this suprathermal electron energy by the estimated volume of the emission ($\sim 10^{66}\,\mathrm{cm}^3$) leads to an energy density of $\sim 0.2\,\mathrm{eV\,cm}^{-3}$, comparable to the Cosmic ray ion energy density of $\sim 1\,\mathrm{eV\,cm}^{-3}$ in the Galaxy (e.g. Wdowczyk & Wolfendale 1989). Therefore, on energetic grounds the LECRe scenario is plausible. The LECRe may be accelerated in supernovae remnants (e.g. Yamasaki et al. 1997) or by ambient interstellar plasma turbulence (Schlickeiser 1997).

We now show that low energy Cosmic ray ions (LECRi) can not contribute significantly to the hard X-ray emission. LECRi which produce nonthermal X-rays via atomic interactions also produce gamma-ray emission and the light elements Li, Be and B via nuclear reactions (Ramaty et al. 1997 and references therein). The calculated 3-7 MeV nuclear gamma-ray line fluxes, and Galaxy-wide Be production rates that would accompany the X-ray emission are shown in Figure 4a and 4b, respectively. For these calculations, we used the same interaction model as Ramaty et al. (1997) and Tatischeff et al. (1998) and an accelerated ion source spectrum also used by these authors,

$$\frac{dN_i}{dt}(E_i) \propto E_i^{-1.5} e^{-E_i/E_{0i}} \ . \tag{6}$$

We employed three different compositions for the LECRi: CRS and $\mathrm{CRS_{metal}}$ (Ramaty et al. 1997) and $\mathrm{OB_{IG}}$ (Parizot, Cassé & Vangioni-Flam 1997). CRS is the composition of the current epoch Galactic cosmic-ray sources; $\mathrm{CRS_{metal}}$ is identical to CRS, but without protons and α particles; $\mathrm{OB_{IG}}$ is the calculated average composition of the stellar winds from OB associations in the inner Galaxy. The calculations are normalized to a nonthermal X-ray production by the fast ions of $2 \times 10^{37}\,\mathrm{erg\,s}^{-1}$ in the 2-9 keV energy range, which is the luminosity of the LECRe component in our best fit model (Table 1). In figure 4a, the

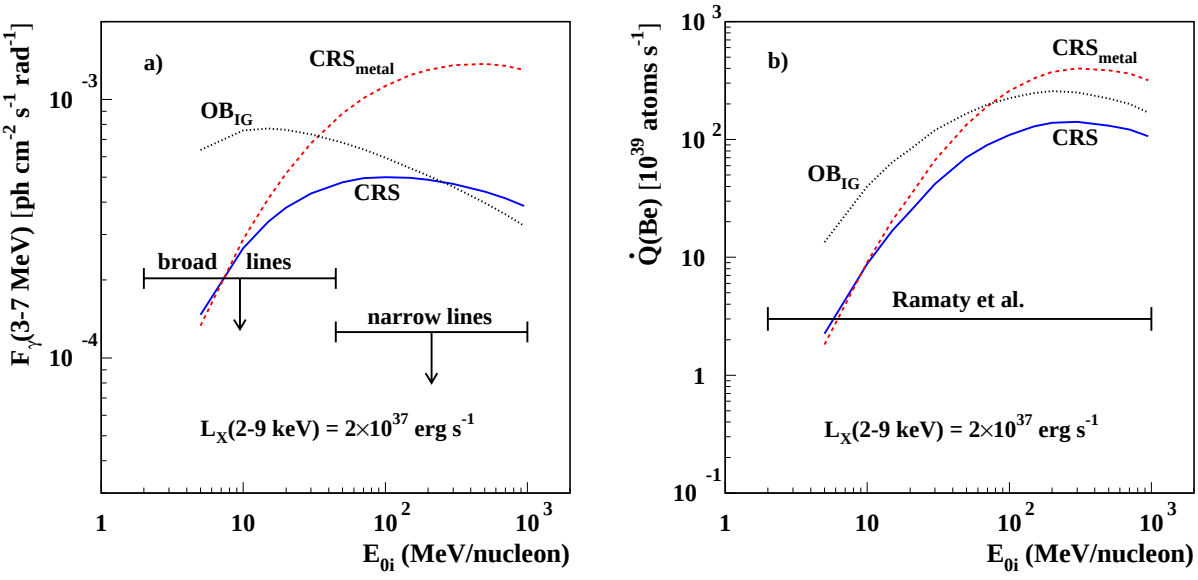

Fig. 4.— (a) Calculated 3-7 MeV nuclear gamma-ray line fluxes from the central radian of the Galaxy (left panel), and (b) predicted Galaxy-wide Be production rates, as a function of E_{0i} (eq. [6]) (right panel). The calculations are normalized to a nonthermal X-ray production by the fast ions of $2 \times 10^{37}\,\mathrm{erg\,s^{-1}}$ in the 2-9 keV energy range. Also shown in panels (a) and (b) are the OSSE upper limits for both broad and narrow line emissions (Harris et al. 1997) and the current epoch Be production rate recommended by Ramaty et al. (1997) and Ramaty et Lingenfelter (1998), respectively.

predicted gamma-ray line fluxes are compared with the upper limits obtained with OSSE for both broad and narrow line emissions from the central radian of the Galaxy (Harris et al. 1997). The $\mathrm{CRS_{metal}}$ composition produces only broad gamma-ray lines, whereas the CRS and $\mathrm{OB_{IG}}$ compositions also produce intense narrow lines, from the interactions of accelerated protons and α particles with ambient ^{12}C and ^{16}O. Thus, only the $\mathrm{CRS_{metal}}$ composition with $E_{0i} \lesssim 7$ MeV/nucleon does not violate the OSSE upper limits (Fig. 4a). Furthermore, it is shown in Figure 4b that the predicted Be production rates significantly exceed the nominal value obtained from the observation of the linear correlation between Be and Fe for [Fe/H]<-1, $\dot{Q}(\mathrm{Be}) = 3 \times 10^{39}$ Be-atoms $\mathrm{s^{-1}}$ (Ramaty et al. 1997, Ramaty & Lingenfelter 1998), with the exception of very low energy ions of $\mathrm{CRS_{metal}}$ or CRS composition. Moreover, nonthermal X-ray production by such very low energy ions is very inefficient. We find that LECRi with $E_{0i} \lesssim 7$ MeV/nucleon should deposit more than $3 \times 10^{42}\,\mathrm{erg\,s^{-1}}$ in the ISM to produce the 2-9 keV luminosity of $2 \times 10^{37}\,\mathrm{erg\,s^{-1}}$, exceeding by more than a factor of 2 the total power delivered by Galactic supernovae, $1.5 \times 10^{42}\,\mathrm{erg\,s^{-1}}$ (Ramaty & Lingenfelter 1998). We thus conclude that LECRi do not significantly contribute to the hard X-ray emission below

10 keV. Using different ion source spectra, Pohl (1998) and Tatischeff, Ramaty & Valinia (1999) have shown that LECRi can not account for the X-ray data above 10 keV either.

Although the resolution of the ASCA data does not allow us to distinguish between purely non-equilibrium ionization and LECRe plus thermal models, we contend that the non-equilibrium ionization models are generally disfavored. This is because the purely thermal models require a very hot gas ($kT \sim 7$ keV) that is uniformly produced and confined in the Galactic disk (a very contrived scenario). On the other hand, the presence of a nonthermal component for the emission is demonstrated by hard X-ray/soft γ-ray observations of the Galactic background (e.g. Yamasaki et al. 1997; Valinia & Marshall 1998; VKM00; Boggs et al. 1999). The LECRe model along with a shock heated plasma component (both of which may have been created in supernovae explosions) provide a plausible explanation for the diffuse Galactic background emission. Observations performed with XMM are expected to be able to distinguish between these scenarios because of its high throughput and CCD spectral resolution.

We thank Keith C. Gendreau for his help in preparing the diffuse ASCA ARF during the early phase of this work. This research has taken advantage of HEASARC archival data base.

REFERENCES

Anders, E., & Grevesse, N. 1989, Geochim. Cosmochim. Acta, 53, 197

Berger, M. J., & Seltzer, S. M. 1982, National Bureau of Standards Rep.: NBSIR 82-2550

Bleach, R. D., Boldt, E. A., Holt, S. S., Schwartz, D. A., & Serlemitsos, P. J. 1972, ApJ, 174, L101

Boggs, S. E., Lin, R. P., Slassi-Sennou, S., Coburn, W., & Pelling, R. M. 1999, astro-ph/9908170

Dogiel, V. A., Ichimura, A., Inoue, H., & Masai, K. 1998, PASJ, 50, 567

Harris, M. J., et al. 1997, in Proc. Fourth Compton Symp., (New York: AIP), 2, 1079

Kaneda, H. 1997, Ph.D. Dissertation, University of Tokyo

Kaneda, H., Makishima, K., Yamauchi, S., Koyama, K., Matsuzaki, K., & Yamasaki, N. Y. 1997, ApJ, 491, 638 (K97)

Kaastra, J. S., 1992, An X-ray Spectral Code for Optically Thin Plasmas (Internal SRON-Leiden Report, updated version 2.0)

Koch, H. W., & Motz, J. W. 1959, Rev. Mod. Phys., 31, 920

Koyama, K., Makishima, K., Tanaka, Y., & Tsunemi, H. 1986, PASJ, 38, 121

Krause, M. O. 1979, J. Phys. Chem. Ref. Data, 8, 307

Long, X., Liu, M., Ho, F., & Peng, X. 1990, Atomic Data and Nucl. Data Tables, 45, 353

Makishima, K. et al. 1996, PASJ, 48, 171

Mewe, R., Gronenschild, E. H. B. M., & van den Oord, G. H. J. 1985, A&AS, 62, 197

Mewe, R., Lemen, J. R., & van den Oord, G. H. J., 1986, A&AS, 65, 511

Ottmann, R., & Schmitt, J. H. M. M. 1992, A&A, 256, 421

Parizot, E. M. G., Cassé, M., & Vangioni-Flam, E. 1997, A&A, 328, 107

Patterson, J. 1984, ApJS, 54, 443

Pohl, M. 1998, A&A, 339, 587

Quarles, C. A. 1976, Phys. Rev. A, 13, 1278

Ramaty, R., Kozlovsky, B., Lingenfelter, R. E., & Reeves, H. 1997, ApJ, 488, 730

Ramaty, R., & Lingenfelter, R. E. 1998, Proceedings of the Meudon Symposium, Galaxy Evolution, Kluwer Academic, in press

Salem, S. I., Panossian, S. L., & Krause, R. A. 1974, Atomic Data and Nucl. Data Tables, 14, 91

Schlickeiser, R. 1997, A&A, 319, L5

Skibo, J. G., & Ramaty, R. 1993, A&AS, 97, 145

Skibo, J. G., Ramaty, R., & Purcell, W. R. 1996, A&AS, 120, 403

Tanaka, Y., Miyaji, & Hasinger 1999, in the proceedings of the 4th ASCA Symposium, in press

Tanuma, S., Yokoyama, T., Kudoh, T., Matsumoto, R., Shibata, K., & Makishima, K. 1999, PASJ, 51, 161

Tatischeff, V., Ramaty, R., & Kozlovsky, B. 1998, ApJ, 504, 874

Tatischeff, V., Ramaty, R., & Valinia, A., 1999, in "LiBeB, Cosmic Rays and Gamma-Ray Line Astronomy", ASP Conference Series, eds. R. Ramaty, E. Vangioni-Flam, M. Cassé and K. Olive, 226

Townes, C. H. 1989, in IAU Symp. 136, The Center of the Galaxy, ed. M. Morris (Dordrecht,: Kluwer), 1

Valinia, A., & Marshall, F. E. 1998, ApJ, 505, 134

Valinia, A., Kinzer, R. L., & Marshall, F. E. 2000, ApJ, 534, 277 (VKM00)

Wdowczyk, J., & Wolfendale, A. W. 1989, Annu. Rev. Nucl. Part. Sci., 39, 43

Yamasaki N. Y. et al. 1997, ApJ, 481, 821

Table 1. Models and Best Fit Parameters to the Galactic X-ray Background Spectrum

Model	Model Parameter	Value
$4-9$ keV; N_H(Mekal + LECRe + CXB[a])		
	N_H	$2.7^{+4.5}_{-2.7}$
Mekal	kT(keV)	$2.8^{+1.2}_{-1.1}$
	Abundances	$1.3^{+1.7}_{-0.5}$
	Flux(%)[b]	38
LECRe	s	0.3
	E_0(keV)	90
	Flux(%)[b]	36
	Total Flux[c]	1.39×10^{-7}
	χ^2/ν	194.8/225
$0.6-9$ keV; N_{H1}(Mekal$_1$ + LECRe + CXB[a]) + N_{H2}(Mekal$_2$)		
	N_{H1}	$3.6^{+0.5}_{-0.7}$
Mekal$_1$	kT(keV)	2.8 ± 0.4
	Abundances	$1.2^{+0.4}_{-0.3}$
	Flux(%)[b]	24
LECRe	s	0.3
	E_0(keV)	90
	Flux(%)[b]	11
	N_{H2}	$1.4^{\pm0.1}$
Mekal$_2$	kT(keV)	$0.56^{+0.02}_{-0.08}$
	Abundances	$0.5^{+0.5}_{-0.1}$
	Flux(%)[b]	57
	Total Flux[c]	9.75×10^{-7}
	Total Luminosity[d]	2.3×10^{38}
	χ^2/ν	491.7/510

[a]The Cosmic X-ray Background (CXB) component (not shown in the table) is frozen in the model with a flux of 6.2×10^{-8} ergs cm^{-2} s^{-1} sr^{-1} in the $2-10$ keV band.

[b]Percentage of the flux of this component to the total flux.

[c]Total unabsorbed flux in the indicated band in ergs cm^{-2} s^{-1} sr^{-1}.

[d]Luminosity in ergs s^{-1} was calculated assuming an emitting volume of 10^{66} cm^{-3} and an average depth of emission of ~ 17 kpc.